



Stochastic variability and transitions to chaos in a hierarchical three-species population model



Irina Bashkirtseva, Lev Ryashko*, Tatyana Ryazanova

Ural Federal University, Lenina, 51, Ekaterinburg 620000, Russian Federation

ARTICLE INFO

Article history:

Received 13 April 2018

Revised 23 December 2018

Accepted 30 December 2018

Available online 15 January 2019

Keywords:

Population dynamics

Noise-induced transitions

Stochastic sensitivity

Chaos

ABSTRACT

A variability of the dynamic behavior in stochastically forced multi-species population models is studied. We address how noise can generate complex oscillatory regimes with transitions between attractors and order-chaos transformations. For the parametric analysis of noise-induced transitions, we utilize a semi-analytical technique based on the stochastic sensitivity analysis of attractors and confidence domains method. This approach is used in the study of the fairly realistic three-species population model describing the interaction of prey, predator and top predator. We consider in detail the parametric zone where the system is monostable with excitable limit cycle, or bistable with coexisting limit cycle and chaotic attractor. These zones are separated by the crisis bifurcation point. Noise-induced transitions between regular and chaotic attractors in the bistability zone are analysed by the confidence ellipses method. In the monostability zone, a mechanism of the transition from regular periodic to multimodal chaotic oscillations is studied.

© 2019 Elsevier Ltd. All rights reserved.

1. Introduction

Complex biological systems naturally arise in the study of interacting populations with several trophic levels. Even in the class of deterministic models of hierarchical population systems with three trophic levels, a great variety of dynamic regimes is observed, both regular (equilibria, cycles) and chaotic (strange attractors). In such models, the nonlinearity of the biological relations can lead to complex local and nonlocal bifurcations [8,9,27]. Here, a multistability often occurs and the dynamic regime is determined not only by the system parameters but also by the choice of initial values. In the multistability zones, regular and chaotic oscillations can coexist. The presence of random perturbations leading to transitions from one attractor to another makes the dynamics more complicated, generating regimes that have no analogues in the initial deterministic models [1,3,4,11,15,18,19,22,23]. Description of the qualitative variety of possible stochastic phenomena in nonlinear population systems and the development of mathematical tools for their constructive parametric analysis is a challenging problem of the modern biological modelling [2,6,7,12,13,20,25].

For the description of stochastic phenomena, methods of the direct numerical simulation of the solutions of the corresponding

stochastic equations are quite sufficient. However, for the clarification of the underlying reasons of such phenomena, it is extremely important to develop theoretical methods to analyze probability distributions of stochastic flows in dependence on the geometry of attractors and their basins of attraction.

In the study of new phenomena in nonlinear dynamical systems and development of methods for their mathematical analysis, an important role is played by sufficiently simple conceptual models. With the help of such models, the main phenomena are illustrated and new approaches to their analysis are demonstrated. In the population dynamics of the prey and predators, the well-known Lotka–Volterra model was one of the first. On the basis of this model, the nature of oscillations in the number of prey and predators has been clarified by the qualitative theory of differential equations. Now more complex models of interacting populations are being developed, taking into account a greater number of trophic levels and various forms of their interrelationships [8,10,17,27].

In the present paper, a tri-trophic “prey-predator-top predator” model [26] is chosen as such a conceptual model. Within the framework of this model, it is possible to cover a wide variety of dynamic regimes, both regular and chaotic, with zones of mono- and bistability. Here, the change in the dynamic regimes is associated with bifurcations of different types, namely saddle-node, Andronov–Hopf, period-doubling, and crisis bifurcations. In the presence of such a variety of attractors and bifurcations in the

* Corresponding author.

E-mail address: lev.ryashko@urfu.ru (L. Ryashko).

deterministic model, random perturbations can lead to the appearance of new phenomena that further complicate the dynamics of the population system.

A rigorous mathematical description of the dynamics of stochastic flows is given by the Fokker–Planck equation [16]. However, a direct use of this equation faces serious technical difficulties even in the two-dimensional case. In these circumstances, approximations based on the quasipotential method and stochastic sensitivity function (SSF) technique can be used [5,14]. The fundamentals of this technique are briefly described in the Appendix. The aim of this paper is to describe the stochastic phenomena observed in the tri-trophic population model in mono- and bistable zones with regular and chaotic attractors. To analyse these phenomena, we apply the method of confidence domains.

In Section 2, attractors and bifurcations in the initial deterministic model are shortly described and zones of mono- and bistability are detected. Here, we show that in bistability zone one of the attractors is the regular stable cycle, and the second attractor (regular or chaotic) belongs to the Feigenbaum's tree. As the control parameter passes the crisis bifurcation, the chaotic attractor disappears, and the system becomes monostable.

Section 3 is devoted to the description of the various stochastic phenomena and their mathematical analysis. In Section 3.1, we present various scenarios of the changes of the stochastic behavior in the bistability zone under increasing noise. Here, noise-induced transitions between regular and chaotic attractors are studied on the basis of SSF technique and confidence ellipses method.

Peculiarities of the noise-induced generation of chaos in the monostability zone where regular stable limit cycle is the single attractor are discussed in Section 3.2.

2. Deterministic model

Consider the three-dimensional nonlinear dynamic system [21,26]

$$\begin{aligned}\dot{x} &= ax - bx^2 - \frac{w_0xy}{x + d_0}, \\ \dot{y} &= -cy + \frac{w_1xy}{x + d_1} - \frac{w_2yz}{y + d_2}, \\ \dot{z} &= dz^2 - \frac{w_3z^2}{y + d_3},\end{aligned}\quad (1)$$

which models the interaction of three species in the food chain “prey – predator – top predator” with Holling-type II functional responses. Here, variables x , y , and z represent corresponding population densities, and all system parameters are positive. The parameter a stands for the prey intrinsic growth rate, the parameter b measures the competition of prey, the parameter c is a mortality of the predator y , and the parameter d describes the growth rate of z . Parameters w_i , d_i ($i = 0, 1, 2, 3$) characterize the Holling-type interactions of species.

In the present paper, we fix system parameters as follows [21]

$$b = 0.06, w_0 = 1, d_0 = 10, c = 1, w_1 = 2,$$

$$d_1 = 10, w_2 = 0.405, d_2 = 10, d = 0.038, w_3 = 1, d_3 = 20$$

and study a variability of system dynamics for the changing parameter a .

For considered parameters, only four equilibria located in the first octant

$$M_0(0, 0, 0), \quad M_1\left(\frac{a}{0.06}, 0, 0\right),$$

$$M_2(10, 20a - 12, 0), \quad M_3(\bar{x}_3, \bar{y}_3, \bar{z}_3)$$

have the biological sense. Here,

$$\begin{aligned}\bar{x}_3 &= \frac{a}{0.12} - 5 + \frac{1}{0.12}\sqrt{(a + 0.6)^2 - 1.52}, \quad \bar{y}_3 = 6.31579, \\ \bar{z}_3 &= -40.3 + 80.6 \frac{\bar{x}_3}{\bar{x}_3 + 10}.\end{aligned}$$

The equilibria M_0, M_1 and M_2 describe the degenerate cases when one or more species are absent. The only non-singular equilibrium M_3 corresponding to the regime of the equilibrium coexistence of all three species has positive coordinates only for $a > 0.9158$. This equilibrium being stable for $0.9158 < a < 1.2966$, loses its stability at the Andronov–Hopf bifurcation point $a = 1.2966$. For $a > 1.2966$, system (1) shows a standard Feigenbaum's cascade of the period-doubling bifurcations with order-chaos transitions. Here, densities of the interacting populations exhibit a complex periodic or chaotic behavior related to the attractors of this Feigenbaum's tree.

A significant change in system (1) behavior occurs at the point $a = 1.7805$ where the second attractor (limit cycle) appears as a result of the saddle-node bifurcation. This stable cycle of larger amplitude coexists with the regular and chaotic attractors of the Feigenbaum's tree. At the point $a = 1.866$, this cycle loses its stability and transforms into the stable 2-cycle. Attractors of the Feigenbaum's tree (blue color) and coexisting limit cycles (red color) are shown in the bifurcation diagram in Fig. 1. Here, z -coordinates of attractors are plotted for $z < 8$, so only lower branches of attractors are presented. Additionally, by black color, boundaries of the basins of attraction of the “blue” and “red” attractors in the Poincaré section $P = \{(x, y, z) | y = \bar{y}_3\}$ are plotted.

As one can see, at the point $a = 1.8916$, the system undergoes a crisis bifurcation: the Feigenbaum's tree touches the separatrix and disappears. System (1) is bistable in the interval $1.7805 < a < 1.8916$, so, the dynamic regime of this population system essentially depends on the initial values of population densities.

A presence of the random noise in systems with coexisting attractors significantly increases the variety of dynamic behavior. Here, it is highly important to understand the mechanisms of noise-induced transitions between basins of attraction and analyse a stochastic preference of the coexisting attractors. In the next sections, we study the stochastic variability of the system (1) in the presence of environmental random disturbances.

3. Stochastic model

Consider model (1) with stochastic disturbances in the parameter a

$$\begin{aligned}\dot{x} &= ax - bx^2 - \frac{w_0xy}{x + d_0} + \varepsilon x\xi(t), \\ \dot{y} &= -cy + \frac{w_1xy}{x + d_1} - \frac{w_2yz}{y + d_2}, \\ \dot{z} &= dz^2 - \frac{w_3z^2}{y + d_3},\end{aligned}\quad (2)$$

where ε is a scalar parameter of the environmental noise intensity and $\xi(t)$ is a scalar white Gaussian noise with parameters $E\xi(t) = 0$, $E\xi(t)\xi(\tau) = \delta(t - \tau)$.

In our analysis of the stochastic variability in system (2), we consider the parametric zone $1.7805 < a < 1.8916$ of bistability, and the monostability zone $a > 1.8916$ near the crisis bifurcation point.

In the bistability zone, “red” limit cycles can coexist with both regular and chaotic attractors. A case when both coexisting attractors are limit cycles is studied in [6]. In the present paper, we focus on the more complex case when the “red” limit cycle coexists with the “blue” chaotic attractor of the Feigenbaum's tree. Various scenarios of the stochastic behavior for this bistability zone

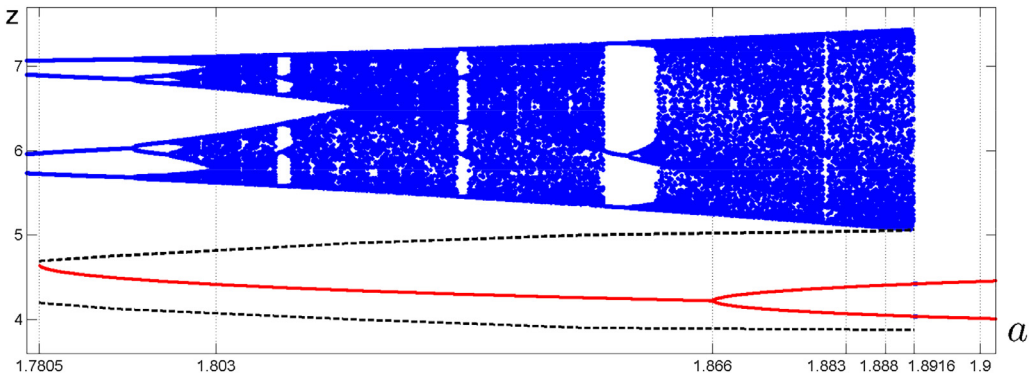


Fig. 1. Bifurcation diagram of system (1).

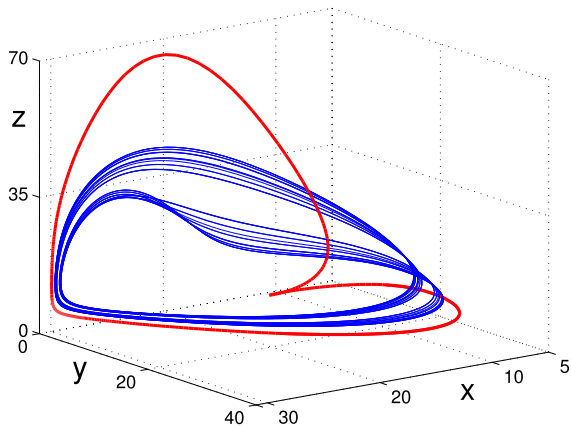


Fig. 2. Attractors of the deterministic system (1) with $a = 1.803$.

are studied in Section 3.1. The effects of noise in the monostability zone $a > 1.8916$ near the crisis bifurcation point are studied in Section 3.2.

3.1. Stochastic transitions between chaotic attractors and cycles

First, consider a case when system (1) possesses coexisting limit 1-cycle and 2-band chaotic attractor. In Fig. 2, 1-cycle (red) and chaotic attractor (blue) are plotted for $a = 1.803$.

Let us study a behavior of the stochastic system under increasing noise. Consider the random trajectories (green) starting from the chaotic attractor (blue). Phase trajectories and corresponding time series are shown in Fig. 3.

Under the weak noise, random trajectories are localized near the unforced chaotic attractor (see Fig. 3a for $\varepsilon = 0.01$). Here, densities of populations exhibit chaotic noisy oscillations. Under increasing noise, random trajectories after some transient time leave the basin of attraction of the chaotic attractor and start to localize near the deterministic cycle (see Fig. 3b for $\varepsilon = 0.02$). Here, the population system transits from the noisy chaotic to regular oscillations. For the larger noise, the stochastic system exhibits more complex regime with mutual transitions between basins of coexisting attractors (see Fig. 3c for $\varepsilon = 0.03$). Here, multimodal oscillations are observed.

For the quantitative justification of the transitions between order and chaos, we will use the largest Lyapunov exponents Λ . A change of the sign of Λ from minus to plus signals about the transition from order to chaos. In Fig. 4, plots of $\Lambda(\varepsilon)$ are shown by red for trajectories starting from the “red” cycle, and by blue for trajectories starting from the “blue” chaotic attractor. For weak noise, these two branches of Λ are separated because of the absence of

noise-induced transitions between coexisting attractors. Note that at first the increasing noise implies the growth of the Lyapunov exponents for chaotic attractor. This means an amplification of the divergence of random trajectories in the stochastic flow. With the further increase of noise, a sharp jump from positive to negative values is observed for the blue curve. For $\varepsilon > 0.015$, the blue curve merges with the red one. Such junction signals about noise-induced transitions from chaotic attractor to the cycle. A slight decrease of both branches means some stabilization of the stochastic flows. The further increase of noise entails a change in the sign of the Lyapunov exponents Λ from minus to plus, and system dynamics becomes totally chaotic regardless of the initial point.

In the study of mechanisms of noise-induced transitions between coexisting attractors, it is important to compare the dispersion of random trajectories near the attractor and the geometry of the corresponding basin of attraction. To analyse exits of random trajectories from the basins of attraction of limit cycles, we will use a method of the confidence domains. For the parametric description of the dispersion of random trajectories in the orthogonal plane (Poincare section), one can use confidence ellipses constructed on the basis of the stochastic sensitivity function.

Let the deterministic system have the T -periodic solution $\bar{x}(t)$ that describes the limit cycle. For this cycle, the stochastic sensitivity T -periodic matrix $W(t)$ allows us to approximate the dispersion of random states at the Poincare plane that is orthogonal to the cycle at the point $\bar{x}(t)$. The matrix W is singular. Non-zero eigenvalues $\mu_1(t), \mu_2(t)$ of this matrix characterize the sensitivity to noise in the directions of the corresponding eigenvectors $v_1(t), v_2(t)$. Eigenvalues and eigenvectors of the matrix W give us a simple analytical description of the dispersion in the form of the confidence ellipse. Note that the confidence domain for the random trajectories arranged around three-dimensional cycle is composed by the family of such confidence ellipses.

For weak noise, all these ellipses belong to the basin of attraction of the limit cycle. Under increasing noise, these ellipses expand, and for some part of the cycle, the ellipses can intersect the separatrix and occupy the basin of attraction of the other coexisting attractor.

Consider now how this technique of confidence ellipses can be used in the analysis of the phenomena presented above. In Fig. 5, results of such analysis are shown for the stochastic system (2) with $a = 1.803$. In Fig. 5a, by green color, we marked the points of the “red” cycle for which confidence ellipses start partially to occupy the basin of attraction of the coexisting “blue” chaotic attractor. In Fig. 5b, for one of the points from the green zone, the Poincare section with confidence ellipses and fragments of basins of attraction is shown. Here, small and large ellipses are plotted for $\varepsilon = 0.01$ (red) and $\varepsilon = 0.03$ (black). The basins of attraction of the “red” cycle and “blue” chaotic attractor are shown by pink and light blue colors, respectively.

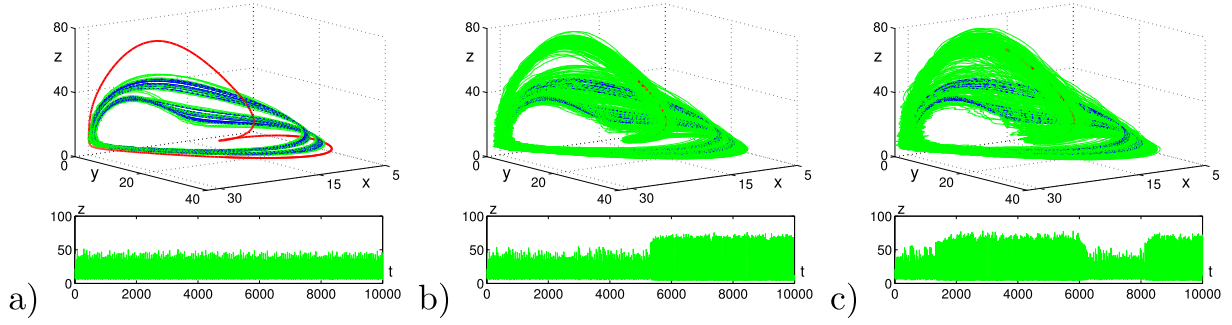


Fig. 3. Stochastic trajectories for $a = 1.803$ with a) $\varepsilon = 0.01$, b) $\varepsilon = 0.02$ and c) $\varepsilon = 0.03$.

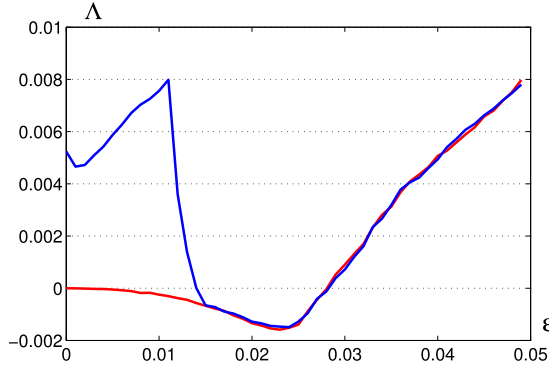


Fig. 4. Largest Lyapunov exponent for system (2) with $a = 1.803$.

As one can see, for $\varepsilon = 0.01$, the confidence ellipse entirely belongs to the basin of attraction of the “red” cycle, and for $\varepsilon = 0.03$, the confidence ellipse partially occupies the basin of attraction of the “blue” chaotic attractor. Using such mutual arrangement of ellipses and basins of attraction, one can predict changes in the behavior of the stochastic system (2) under increasing noise. Indeed, for $\varepsilon = 0.01$, the random trajectories are localized near the deterministic “red” cycle, and for $\varepsilon = 0.03$, random trajectories transits to the “blue” chaotic attractor. Note that this prediction is in a good agreement with the results of the direct numerical simulation shown in Fig. 3.

Now, consider a behavior of the stochastic population model (2) on the right side of the a -interval of the bistability. For $a = 1.888$, the deterministic system has coexisting attractors: “red” 2-cycle and “blue” 1-band chaotic attractor (see Fig. 6).

In Fig. 7, for various values of the noise intensity, random trajectories starting from the chaotic attractor are plotted by green

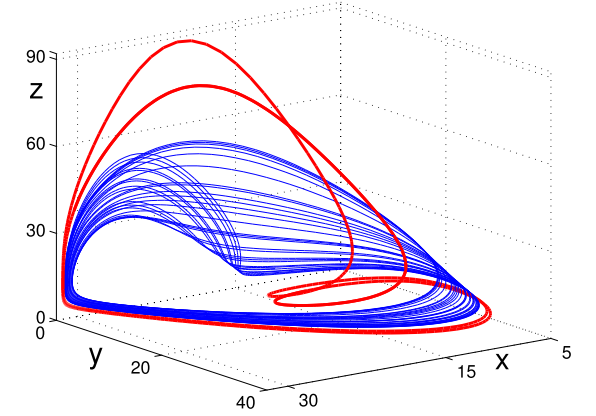


Fig. 6. Attractors of the deterministic system (1) with $a = 1.888$.

color. For weak noise, random trajectories are localized near the initial chaotic attractor (left) and the initial 2-cycle (right) (see Fig. 7a for $\varepsilon = 0.001$). Here, the population system demonstrates noisy chaotic or regular oscillations. Under increasing noise, random trajectories starting from the chaotic attractor after some transient time fall into the basin of attraction of the “red” 2-cycle and further concentrate near this deterministic cycle (see Fig. 7b for $\varepsilon = 0.01$). Here, the population system transits to noisy large-amplitude oscillations. Note that the amplitude of these stochastic oscillations is close to the amplitude of the deterministic 2-cycle oscillations. With increase of noise, the mutual transitions between coexisting deterministic attractors with the multimodal oscillations are observed (see Fig. 7c for $\varepsilon = 0.05$).

For the considered here value $a = 1.888$, it can be seen from Fig. 7 that system (2) demonstrates the preference of the “red” 2-

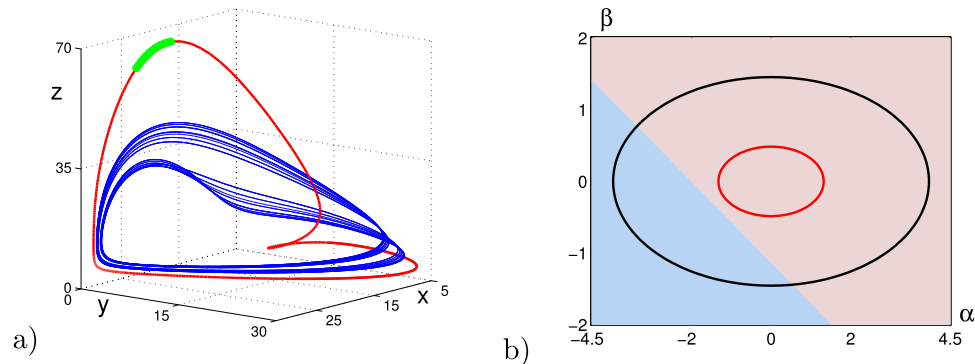


Fig. 5. Stochastic system with $a = 1.803$: a) deterministic attractors with the critical zones marked by green color; b) confidence ellipses for $\varepsilon = 0.01$ (red) and $\varepsilon = 0.03$ (black). (For interpretation of the references to color in this figure legend, the reader is referred to the web version of this article.)

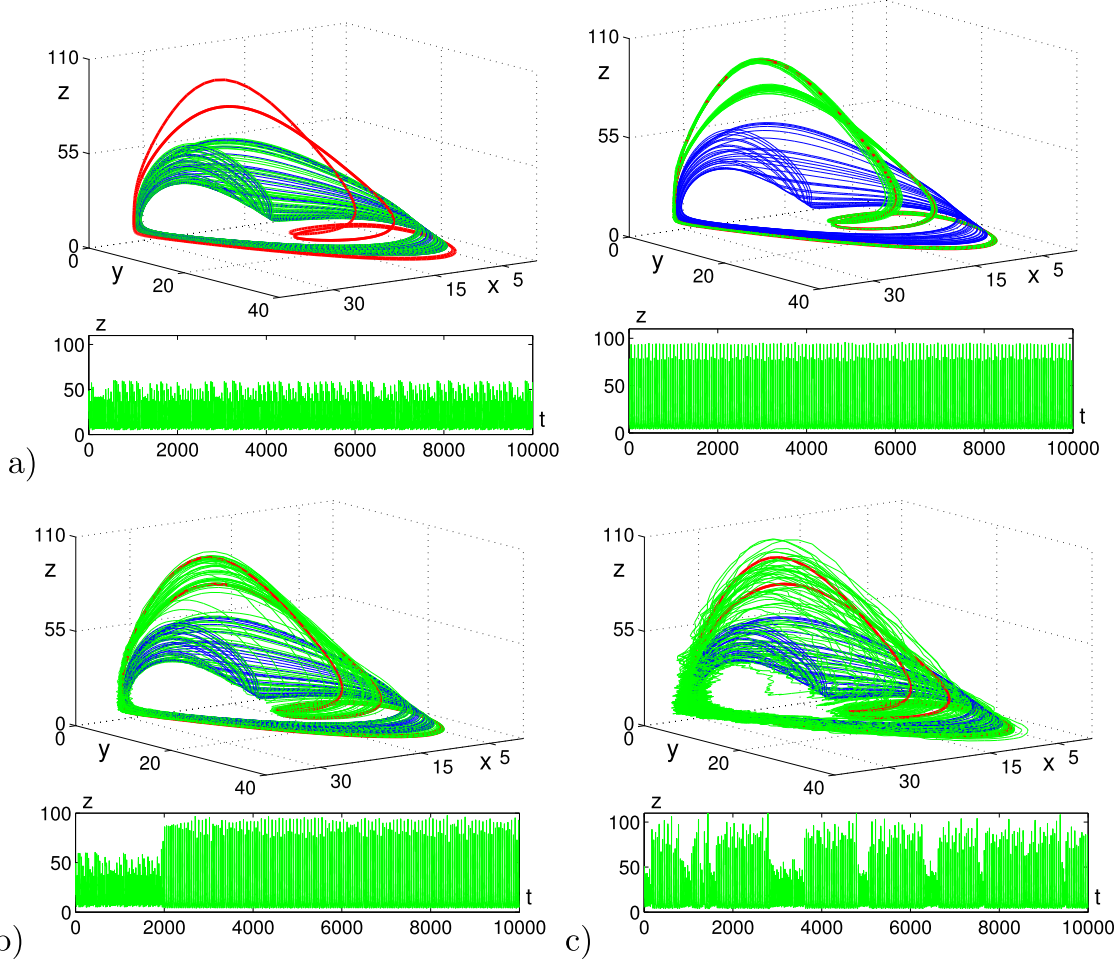


Fig. 7. Stochastic trajectories for $a = 1.888$ with a) $\epsilon = 0.001$, b) $\epsilon = 0.01$ and c) $\epsilon = 0.05$.

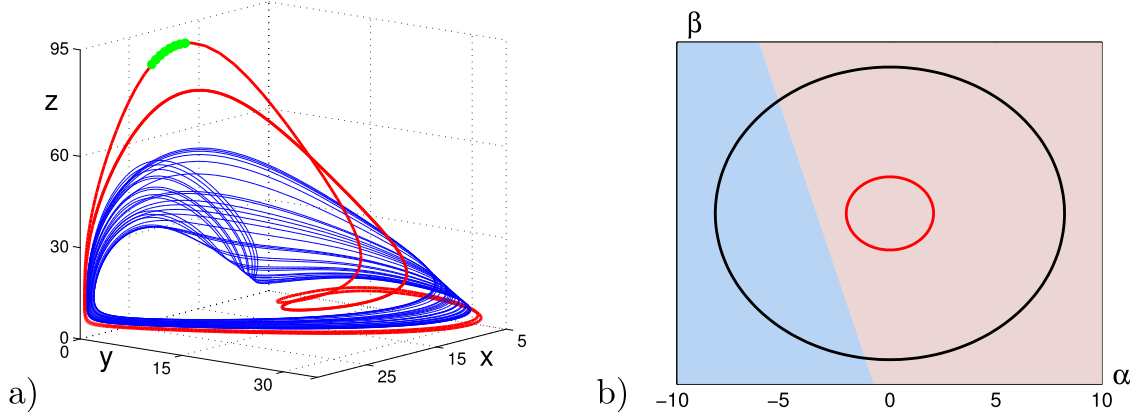


Fig. 8. Stochastic system with $a = 1.888$: a) deterministic attractors with the critical zones marked by green color; b) confidence ellipses for $\epsilon = 0.005$ (red) and $\epsilon = 0.02$ (black). (For interpretation of the references to color in this figure legend, the reader is referred to the web version of this article.)

cycle. Indeed, for the onset of the noise-induced transitions from the “red” 2-cycle to the “blue” chaotic attractor, the stronger noise is required in comparison with the inverse transitions.

Consider now how SSF technique and method of confidence ellipses can be used for the prediction of the noise-induced transitions from the “red” 2-cycle to the “blue” chaotic attractor. Results of this approach are presented in Fig. 8. In Fig. 8a, similar to Fig. 5a, we marked by green color the critical zone. In Fig. 8b, for one of the points from this critical zone, the Poincaré section with confidence ellipses and fragments of basins of attraction is shown.

Here, small and large ellipses are plotted for $\epsilon = 0.005$ (red) and $\epsilon = 0.02$ (black), and basins of attraction of the “red” 1-cycle and “blue” chaotic attractor are shown by pink and light blue colors.

Analysing the mutual arrangement of the confidence ellipses and basins of attraction, one can conclude that for $\epsilon = 0.005$ in the system (2) the “red” 2-cycle dominates, and for $\epsilon = 0.02$, mutual noise-induced transitions between coexisting attractors occur.

In Fig. 9, plots of the largest Lyapunov exponent $\Lambda(\epsilon)$ are shown by red for trajectories starting from the “red” 2-cycle, and by blue for trajectories starting from the “blue” chaotic attractor. As

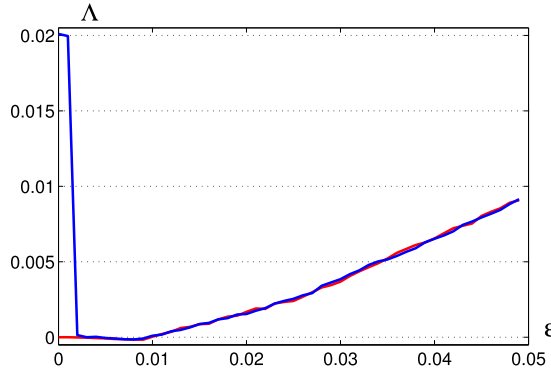
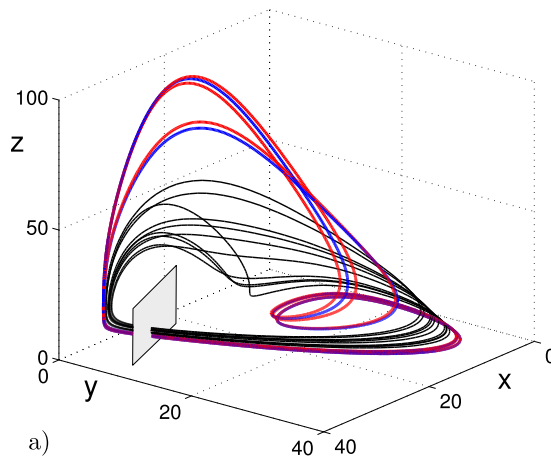
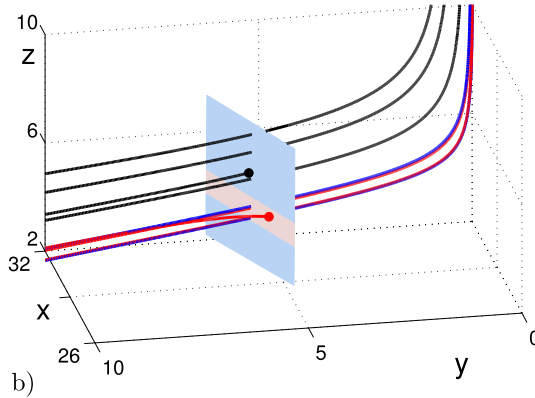


Fig. 9. Largest Lyapunov exponent for system (2) with $a = 1.888$.



a)



b)

Fig. 10. Phase trajectories of the deterministic system (1) for $a = 1.9$: stable limit cycle (blue), subthreshold trajectory (red), superthreshold trajectory (black). (For interpretation of the references to color in this figure legend, the reader is referred to the web version of this article.)

a result of the noise-induced mutual transitions between regular (2-cycle) and chaotic attractors, these curves merge at $\varepsilon = 0.003$, and system displays the chaotic dynamics independently on the initial values.

The examples presented above illustrate cases when in the stochastic system one of the coexisting attractors dominates. Indeed, for both cases $a = 1.803$ and $a = 1.888$, just after the merge of branches of Lyapunov exponents, the dominant is the regular attractor (cycle). In both cases, the scenario of noise-induced transformations of system dynamics is qualitatively similar. Nevertheless, it should emphasize the difference. Indeed, for $a = 1.803$,

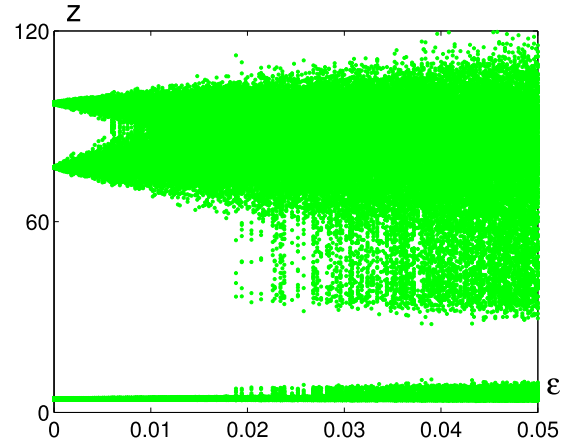


Fig. 11. Stochastic system (2) with $a = 1.9$: z -coordinates of random states in the Poincare section $P = \{(x, y, z) | y = \bar{y}_3\}$.

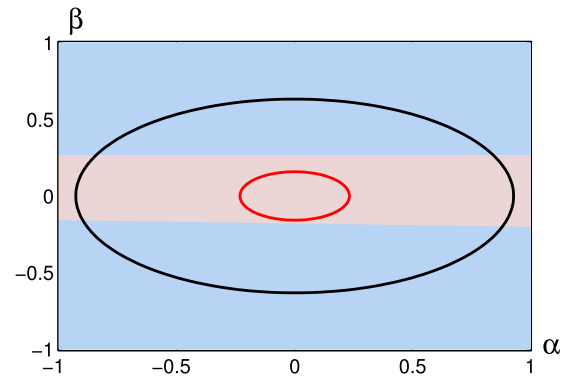


Fig. 12. Subthreshold (pink) and superthreshold (light blue) zones of the deterministic system (1) and confidence ellipses for stochastic system (2) with $\varepsilon = 0.005$ (red) and $\varepsilon = 0.02$ (black). Here $a = 1.9$. (For interpretation of the references to color in this figure legend, the reader is referred to the web version of this article.)

a merge of the branches of Lyapunov exponents is observed for larger noise than for $a = 1.888$. Correspondingly, the onset chaos for mixed-mode stochastic oscillations occurs also for larger noise intensity (compare Figs. 4 and 9). So, under increase of the parameter a , the population system becomes more sensitive to noise. In the next part of the paper, we consider the consequences of the transition of the parameter a through the crisis bifurcation point $a = 1.8916$.

3.2. Noise-induced generation of chaos in the monostable regular zone

Consider now the parametric zone $a > 1.8916$ where deterministic system (1) is monostable. To illustrate stochastic effects in this zone we will fix $a = 1.9$. System (1) with $a = 1.9$ has the stable 2-cycle as a single attractor. The phase trajectory of this cycle is shown by blue in Fig. 10a. For any initial point, the trajectories of system (1) tend to this cycle as time tends to infinity but there are two types of the transient processes. Indeed, for small subthreshold deviation of the initial point from the cycle, the trajectory monotonically tends to the cycle (see red curve in Fig. 10). If the initial deviation is larger than some threshold value, then the trajectory at first goes away the cycle, and begins to converge to the cycle after this outlying loop. The fragment of such superthreshold phase trajectory is shown in Fig. 10b by black color. Initial points corresponding to the sub- and superthreshold regimes are shown

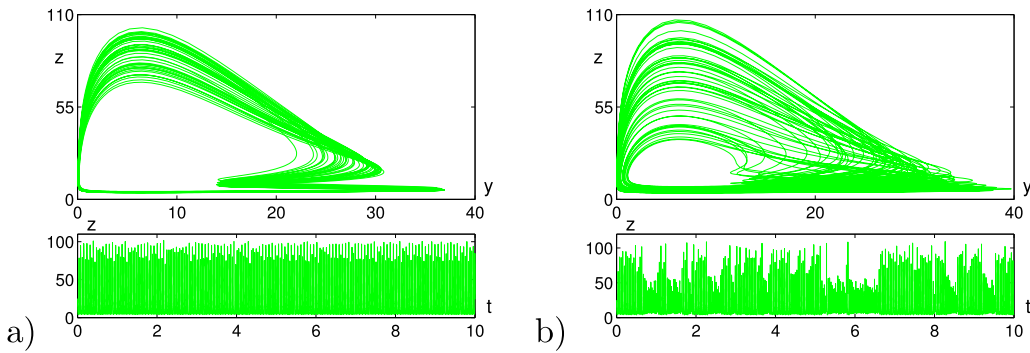


Fig. 13. Stochastic system (2) with $a = 1.9$: y , z -coordinates of phase trajectories and time series of z -coordinates for a) $\varepsilon = 0.01$, b) $\varepsilon = 0.05$.

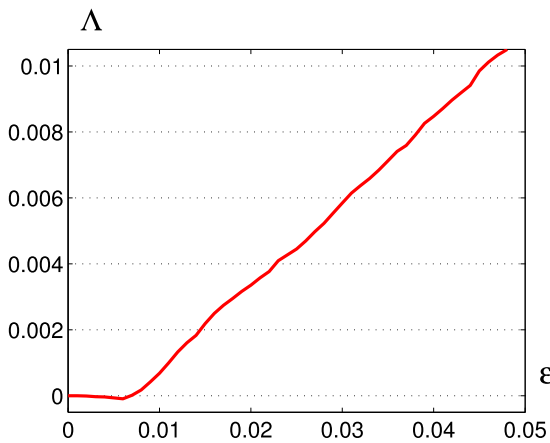


Fig. 14. Largest Lyapunov exponent $\Lambda(\varepsilon)$ for the system (2) with $a = 1.9$.

for some Poincare plane in Fig. 10b by pink and light blue colors respectively.

Consider now how such peculiarities of the phase portrait of the deterministic system are related to the dynamics of the stochastic system (2). In Fig. 11, z -coordinates of random trajectories starting from the deterministic cycle in the Poincare section $P = \{(x, y, z) | y = \bar{y}_3\}$ are plotted versus noise intensity ε . For weak noise, random states belong to the subthreshold zone and exhibit stochastic oscillations near deterministic cycle. The increasing noise results in the increase of their dispersion. However, in Fig. 11, one can see a sharp jump of the dispersion at some noise intensity. The underlying reason of such jump of the dispersion is the fact that stochastic trajectories fall into the superthreshold zone where trajectories move away from the deterministic cycle.

A parametric analysis of the transition from sub- to superthreshold regime of stochastic oscillations in system (2) can be carried out on the basis of the confidence ellipses technique. In Fig. 12, in some Poincare section, fragments of the sub- and superthreshold domains of initial points of the deterministic system (1) are plotted along with the confidence ellipses of the stochastic system (2) with the noise intensity $\varepsilon = 0.005$ (red) and $\varepsilon = 0.02$ (black). For $\varepsilon = 0.005$, the ellipse totally belongs to the subthreshold zone, and for $\varepsilon = 0.02$, some part of the ellipse lies in the superthreshold zone. As one can see, the mutual arrangement of the confidence ellipses and sub- and superthreshold zones is in a good agreement with results of the direct numerical simulations presented in Fig. 11.

As it is shown in Fig. 13, the transition from sub- to superthreshold regime essentially changes amplitude properties of the time series. Dynamics in the superthreshold regime looks like chaotic. To confirm this, we calculated the largest Lyapunov expo-

nent $\Lambda(\varepsilon)$ (see Fig. 14). Here, $\Lambda(\varepsilon)$ increases and becomes positive. So, in the considered here monostability zone where the deterministic system exhibits the single regular attractor (stable 2-cycle), the increasing noise transfers the system from order to chaos.

4. Conclusion

On the example of the conceptual three-dimensional population model, we have shown that the stochastic variability of dynamic regimes is defined by the geometric peculiarities of attractors, basins of attraction and also their stochastic sensitivity. Using the stochastic sensitivity functions, one can construct confidence domains describing the dispersion of random states around initial deterministic attractors. Our semi-analytical approach based on the analysis of the mutual arrangement of confidence domains and borders of basins of attraction gives us a mathematical tool for the constructive analysis of noise-induced transitions and generation of chaos in complex mono- and multistable systems of high dimensions.

Acknowledgments

The work was supported by Russian Science Foundation (N 16-11-10098).

Appendix

In the present paper, for the description of the dispersion of random trajectories of the 3D stochastic population model around the deterministic cycle, a method of confidence ellipses is used. Here, we shortly discuss this method for the general nonlinear stochastic system

$$\dot{x} = f(x) + \varepsilon \sigma(x) \xi(t), \quad (3)$$

where x is an n -vector, $f(x)$ is a n -vector function, $\xi(t)$ is an m -dimensional standard white Gaussian noise with parameters $\langle \xi(t) \rangle = 0$, $\langle \xi(t) \xi^\top(\tau) \rangle = \delta(t - \tau) I$, ε is the scalar parameter of the noise intensity, and $\sigma(x)$ is an $n \times m$ -matrix-valued function of the random disturbances. It is assumed that system (3) with $\varepsilon = 0$ has an exponentially stable limit cycle Γ defined by a T -periodic solution $x = \bar{x}(t)$. Let Π_t be a hyperplane that is orthogonal to Γ at the point $\bar{x}(t)$ ($0 \leq t < T$).

The function $\rho(x, \varepsilon)$ of the stationary probabilistic distribution of random states of system (3) around the deterministic attractor is governed by the Fokker–Planck equation [16]. For the approximation of this function, the asymptotics based on the quasipotential $v(x) = -\lim_{\varepsilon \rightarrow 0} \varepsilon^2 \log \rho(x, \varepsilon)$ are widely used [14]. So, one can write

$$\rho(x, \varepsilon) \approx K \cdot \exp \left(-\frac{v(x)}{\varepsilon^2} \right).$$

For small noise, in a vicinity of the stable deterministic cycle Γ , a constructive approach using the approximation of the quasipotential near the deterministic attractor has been elaborated in [24]. This approach was effectively used in the analysis of various noise-induced transitions [5,6].

In the Poincare section Π_t , the quasipotential can be approximated by the quadratic function:

$$v(x) \approx \frac{1}{2}(x - \bar{x}(t), W^+(t)[x - \bar{x}(t)]).$$

Thus, one can write the corresponding Gaussian approximation of the stationary probabilistic distribution

$$\rho_t(x, \varepsilon) \approx K \exp\left(-\frac{(x - \bar{x}(t), W^+(t)(x - \bar{x}(t)))}{2\varepsilon^2}\right)$$

with the mean value $m_t = \bar{x}(t)$ and covariance matrix $\text{cov}_t := D(t, \varepsilon) = \varepsilon^2 W(t)$. Here, the matrix function $W(t)$ is singular, a sign "+" means a pseudoinversion.

The stochastic sensitivity matrix $W(t)$ is a unique solution of the following differential Lyapunov equation

$$\dot{W} = F(t)W + WF^\top(t) + Q(t)S(t)Q(t)$$

with boundary conditions

$$W(0) = W(T), \quad W(T)r(t) \equiv 0.$$

Here, $F(t) = \frac{\partial f}{\partial x}(\bar{x}(t))$, $S(t) = \sigma(\bar{x}(t))\sigma^\top(\bar{x}(t))$, $r(t) = f(\bar{x}(t))$, $Q(t)$ is a symmetric matrix of the orthogonal projection onto the hyperplane Π_t .

For three-dimensional case, the constructive method for the solution of this boundary problem based on the singular decomposition of the stochastic sensitivity matrix is described in [5]. Using the eigenvalues $\mu_1(t)$, $\mu_2(t)$ and normalized eigenvectors $u_1(t)$, $u_2(t)$ of the stochastic sensitivity matrix $W(t)$, in the plane Π_t , one can construct a confidence ellipse

$$\frac{\alpha^2}{\mu_1(t)} + \frac{\beta^2}{\mu_2(t)} = -2\varepsilon^2 \ln(1 - P). \quad (4)$$

Here, $\alpha = (x - \bar{x}(t), u_1(t))$, $\beta = (x - \bar{x}(t), u_2(t))$ are coordinates of this ellipse in the basis u_1 , u_2 , and P is a fiducial probability.

References

- [1] Anishchenko VS, Astakhov VV, Neiman AB, Vadivasova TE, Schimansky-Geier L. Nonlinear dynamics of chaotic and stochastic systems: tutorial and modern development. Berlin, Heidelberg: Springer-Verlag; 2007. doi:[10.1007/978-3-540-38168-6](https://doi.org/10.1007/978-3-540-38168-6).
- [2] Assaf M, Meerson B. WKB theory of large deviations in stochastic populations. *J Phys A* 2017;50:263001. doi:[10.1088/1751-8121/aa669a](https://doi.org/10.1088/1751-8121/aa669a).
- [3] Barbera AL, Spagnolo B. Spatio-temporal patterns in population dynamics. *Physica A* 2002;314:120–4. doi:[10.1016/S0378-4371\(02\)01173-1](https://doi.org/10.1016/S0378-4371(02)01173-1).
- [4] Barbera AL, Spagnolo B. Role of the noise on the transient dynamics of an ecosystem of interacting species. *Physica A* 2002;315:114–24. doi:[10.1016/S0378-4371\(02\)01245-1](https://doi.org/10.1016/S0378-4371(02)01245-1).
- [5] Bashkirtseva I, Chen G, Ryashko L. Analysis of stochastic cycles in the chen system. *Int J Bifurcation Chaos* 2010;20:1439–50.
- [6] Bashkirtseva I, Ryashko L, Ryazanova T. Analysis of noise-induced bifurcations in the stochastic tritrophic population system. *Int J Bifurcation Chaos* 2017;27:1750208. doi:[10.1142/S021827411750208X](https://doi.org/10.1142/S021827411750208X).
- [7] Bashkirtseva I, Ryashko L. Noise-induced shifts in the population model with a weak allee effect. *Physica A* 2018;491:28–36. doi:[10.1016/j.physa.2017.08.157](https://doi.org/10.1016/j.physa.2017.08.157).
- [8] Bazykin AD. Nonlinear dynamics of interacting populations. World Scient 1998.
- [9] Blasius B, Kurths J, Stone L. Complex population dynamics: nonlinear modeling in ecology, epidemiology and genetics. World Scient 2007.
- [10] Castellanos V, Chan-Lopez RE. Existence of limit cycles in a three level trophic chain with Lotka Volterra and Holling type II functional responses. *Chaos, Solitons Fractals* 2017;95:157–67. doi:[10.1016/j.chaos.2016.12.011](https://doi.org/10.1016/j.chaos.2016.12.011).
- [11] Ciechi S, de Pasquale F, Spagnolo B. Nonlinear relaxation in the presence of an absorbing barrier. *Phys Rev E* 1993;47:3915–26.
- [12] Chesson P. Stochastic population models. In: Kolasa J, Pickett STA, editors. Ecological heterogeneity, vol. 86; 1991. p. 123–43. Ecological Studies: Analysis and Synthesis.
- [13] Dobramysl U, Mobilia M, Pleimling M, Täuber UC. Stochastic population dynamics in spatially extended predator-prey systems. *J Phys A* 2018;51:063001. doi:[10.1088/1751-8121/aa95c7](https://doi.org/10.1088/1751-8121/aa95c7).
- [14] Freidlin MI, Wentzell AD. Random perturbations of dynamical systems. New York/Berlin: Springer-Verlag; 1984.
- [15] Gao JB, Hwang SK, Liu JM. When can noise induce chaos? *Phys Rev Lett* 1999;82:1132–5. doi:[10.1084/j.1600-0706.2003.12387.x](https://doi.org/10.1084/j.1600-0706.2003.12387.x).
- [16] Gardiner CW. Handbook of stochastic methods for physics, chemistry, and the natural sciences. Berlin: Springer-Verlag; 1983.
- [17] Hastings A, Powell T. Chaos in a three-species food chain. *Ecology* 1991;72:896–903. doi:[10.2307/1940591](https://doi.org/10.2307/1940591).
- [18] Horsthemke W, Lefever R. Noise-Induced transitions. Berlin: Springer; 1984.
- [19] Lai YC, Tel T. Transient chaos: complex dynamics on finite time scales. Springer; 2011. doi:[10.1007/978-1-4419-6987-3](https://doi.org/10.1007/978-1-4419-6987-3).
- [20] Lande R, Engen S, Saether BE. Stochastic population dynamics in ecology and conservation. Oxford: Oxford University Press; 2003. doi:[10.1093/acprof:oso/9780198525257.001.0001](https://doi.org/10.1093/acprof:oso/9780198525257.001.0001).
- [21] Letellier C, Aziz-Alaoui MA. Analysis of the dynamics of a realistic ecological model. *Chaos, Solitons Fractals* 2002;13:95–107. doi:[10.1016/S0960-0799\(00\)00239-3](https://doi.org/10.1016/S0960-0799(00)00239-3).
- [22] Liu M, Wang K. Persistence and extinction of a single-species population system in a polluted environment with random perturbations and impulsive toxicant input. *Chaos, Solitons Fractals* 2012;45:1541–50. doi:[10.1016/j.chaos.2012.08.011](https://doi.org/10.1016/j.chaos.2012.08.011).
- [23] McDonnell MD, Stocks NG, Pearce CEM, Abbott D. Stochastic resonance: from suprathreshold stochastic resonance to stochastic signal quantization. Cambridge University Press; 2008. doi:[10.1080/00107510903318814](https://doi.org/10.1080/00107510903318814).
- [24] Mil'shtein GN, Ryashko LB. A first approximation of the quasipotential in problems of the stability of systems with random non-degenerate perturbations. *J Appl Math Mech* 1995;59:47–56. doi:[10.1016/0021-8928\(95\)00006-B](https://doi.org/10.1016/0021-8928(95)00006-B).
- [25] Spagnolo B, Valenti D, Fiasconaro A. Noise in ecosystems: a short review. *Math Biosci Eng* 2004;1:185–211. doi:[10.3934/mbe.2004.1.185](https://doi.org/10.3934/mbe.2004.1.185).
- [26] Upadhyay RK, Rai V. Why chaos is rarely observed in natural populations. *Chaos, Solitons Fractals* 1997;8:1933–9.
- [27] van Voorn GAK, Kooi BW, Boer MP. Ecological consequences of global bifurcations in some food chain models. *Math Biosci* 2010;226:120–33. doi:[10.1016/j.mbs.2010.04.005](https://doi.org/10.1016/j.mbs.2010.04.005).